A. HEIDARI, F. GHORBANI, M. GHORBANI
Institute for Advanced Studies
(Tehran 14456-63543, Iran; e-mail: mohammadalighorbani1983@yahoo.com)

A NEW METHOD FOR INVESTIGATING AND ACCURATELY SOLVING THE ONE-DIMENSIONAL QUANTUM ISING MODEL IN CONSTANT AND VARIABLE TRANSVERSE MAGNETIC FIELDS

PACS 11.10.-z, 13.40.-f, 13.90.+i

The one-dimensional quantum Ising model (1D QIM) simply shows quantum phase transitions (QPTs) at the nearest neighbor interactions in a constant magnetic field. Many methods have been heretofore devised to accurately solve 1D QIM. Here, by employing the continuous unitary transformation as a new analytical method for solving many-particle systems, 1D QIM is first solved in the case of a constant transverse magnetic field and a regular variable (periodic) transverse magnetic field. As expected, the critical exponents obtained from the accurate solution to these two models are the same as continuous unitary transformation's results. Moreover, through the Padé approximation and the high-temperature series expansion, we study the susceptibility of an Ising zero-field system to the antiferromagnetic interaction on a kagome lattice. In this model, by assigning various values to the antiferromagnetic interaction constant, the phase transition appears for $J_{\rm AF}/J_{\rm F} > -0.5$. According to the universality theory, such systems' critical exponent is well consistent with that in the Ising model.

K e y w o r d s: quantum Ising model (1D QIM), quantum phase transitions, Padé approximation, antiferromagnetic interaction.

1. Introduction

The QIM with the nearest neighbor interaction in the constant transverse magnetic field $-Jg\sigma_n^x$ is defined through [1]:

$$H = -J\sum_n \left(g\sigma_n^x + \sigma_n^z\sigma_{n+1}^z\right), \tag{1}$$

where $J > 0$ is the coupling constant of ferromagnetic interaction, $g > 0$ is a dimensionless constant adjustable for creating a QPT in this model, and σ_n^x and σ_n^z are Pauli's matrices satisfying the commutative relation

$$\left[\sigma_n^\alpha, \sigma_m^\beta\right] = 2i\delta_{nm}\varepsilon_{\alpha\beta\gamma}\sigma_n^\gamma, \tag{2}$$

where $\{\alpha,\beta,\gamma\} = \{x,y,z\}$, δ_{nm} is the Kronecker delta function, $\varepsilon_{\alpha\beta\gamma}$ is the Levi–Civita exponent, and the indices m and n denote sites. In this Hamiltonian, the constant magnetic field $-Jg\sigma_n^x$ affects spin states along the z-axis and perturbs a spin regularity along this direction through inversing spins

$$\sigma^x\left|\uparrow\right\rangle = \left|\downarrow\right\rangle, \quad \sigma^x\left|\downarrow\right\rangle = \left|\uparrow\right\rangle. \tag{3}$$

The second term in (1) represents the ferromagnetic interaction between two neighboring spins. This term causes a magnetic order in the system. Therefore, the competition between the ferromagnetic coupling constants J and the magnetic field $-Jg\sigma_n^x$ determines this system's phase.

In the limit $g \gg 1$, the first term in (1) is dominant, and the system's ground state is almost the

paramagnetic state, in which spins are oriented along the directions $+x$ and $-x$:

$$|\psi_{gs}\rangle = |\rightarrow\rangle\,|\rightarrow\rangle \ldots |\rightarrow\rangle\,|\rightarrow\rangle\,, \tag{4}$$

$$|\psi_{gs}\rangle = |\leftarrow\rangle\,|\leftarrow\rangle \ldots |\leftarrow\rangle\,|\leftarrow\rangle\,, \tag{5}$$

where it is expected that

$$|\rightarrow\rangle = \frac{1}{\sqrt{2}}\left(|\uparrow\rangle + |\downarrow\rangle\right), \tag{6}$$

$$|\leftarrow\rangle = \frac{1}{\sqrt{2}}\left(|\uparrow\rangle - |\downarrow\rangle\right). \tag{7}$$

In the limit $g \ll 1$, the first term in (1) is negligible in comparison with the second one such that the QIM Hamiltonian is reduced to $H \approx -J\sum_n \sigma_n^z \sigma_{n+1}^z$. In this limit, the system's ground state is almost ferromagnetic in which all the spins are along $+z$ and $-z$:

$$|\psi_{gs}\rangle = \prod_n |\uparrow\rangle_n, \tag{8}$$

$$|\psi_{gs}\rangle = \prod_n |\downarrow\rangle_n. \tag{9}$$

It is evident that the system has a double degeneracy selecting only one of the above states as the ground state in the thermodynamic limit (symmetry spontaneous breaking). Accordingly, when the parameter g is activated and increased from zero to the values much larger than 1, a quantum phase transition occurs from ferromagnetic phase to paramagnetic phase at the critical point $g = g_c$.

The another point that the 1D QIMs in $-Jg\sigma_n^x$ and $(-1)^n Jg\sigma_n^x$ are simply converted to each other by a 180° rotation for even and odd spins.

In this paper, this model in $-Jg\sigma_n^x$ and $(-1)^n Jg\sigma_n^x$ is precisely solved employing continuous unitary transformations (CUTs) [2–6], and its energy spectrum, quantum critical point g_c, and critical exponent $z\nu$ are obtained [14–20]. Since these two models are converted to each other under a 180° rotation, it is expected that we obtain the same critical exponent by accurately solving these two models [9–13]. The Ising model is the simplest and most popular spin system of statistical mechanics. This model can appropriately describe various phenomena such as magnetic matters, gas-liquid coexistence, and bimetallic alloys. This model is used to study a system's phase transitions and was first proposed by Lenz and Ising in 1925 as a ferromagnetic model [33–37]. Ising showed in his PhD thesis that this model does not indicate any phase transition in one dimension [33, 38]. By the first calculations of zero-field free energy in 1944 and the calculation of simultaneous magnetization in 1952, this model's second-order phase transition was proved in two dimensions [37]. The 1D and 2D solutions (in the absence of external fields) to the Ising model can be used to determine the critical exponents of the systems belonging to these two universality classes. Based on the universality theory, the 2D Ising model critical exponents with first-neighbor interactions are the same as those obtained from exactly solving the square-lattice Ising model [39–42].

2. Continuous Unitary Transformations

In 1994, the continuous unitary transformation (or flow equations) method was devised and proposed in the fundamental particle physics by Glazek and Wilson [2] and separately in condensed matter physics by Wegner [3]. The main idea of this method is to use an infinite number of ultrafine unitary transformations that rescale the Hamiltonian's parameters, and the system's Hilbert-space dimension remains completely unchanged [21–23].

In this method, an infinite number of ultrafine unitary transformations are required to diagonalize the Hamiltonian matrix, and a generator is required to generate unitary matrices. If $U(B)$ is the unitary transformation matrix and B is the flow parameter, the transformed Hamiltonian of the system is obtained as

$$H\left(B\right) = U\left(B\right) HU(B)^{\dagger}. \tag{10}$$

By differentiating (10) with respect to B, the Hamiltonian evolution of $H(B)$ can be rewritten as the differential equation given below (flow equation) [4, 5]:

$$\frac{dH\left(B\right)}{dB} = \left[\eta\left(B\right), H\left(B\right)\right], \tag{11}$$

where

$$\eta\left(B\right) = \frac{dU\left(B\right)}{dB} U(B)^{\dagger} = -\eta(B)^{\dagger}, \tag{12}$$

$\eta(B)$ is anti-Hermitian, and represents the unitary matrix generator. A selection for $\eta(B)$ is defined as $\eta(B) = [H_d, H_{nd}]$ [4,5], where H_d and H_{nd} denote the

diagonal and non-diagonal parts of the Hamiltonian, respectively. In this method, because the aim is to diagonalize the Hamiltonian under an infinite number of unitary transformations, the non-diagonal part of the Hamiltonian tends to zero as $B \to \infty$, and the rescaled diagonal part of the Hamiltonian will only remain [24–32].

Another point is that, to obtain the expected values of operators by this method, it is enough to calculate the operators' flow:

$$\frac{dO(B)}{dB} = [\eta(B), O(B)]. \tag{13}$$

Then, using the final eigenstates of the flow Hamiltonian $H(B=\infty)$, the expected values of the operators are obtained [4] as

$$\langle O(B=0)\rangle_{gs}^{B=0} = \langle \Psi_{gs} | O(B=0) | \Psi_{gs}\rangle =$$

$$= \left\langle \Psi_{gs} \left| U^{\dagger}(\infty) U(\infty) O(B=0) U^{\dagger}(\infty) U(\infty) \right| \Psi_{gs} \right\rangle =$$

$$= \left\langle \Psi_{gs} \left| U^{\dagger}(\infty) O(B=0) U(\infty) \right| \Psi_{gs} \right\rangle =$$

$$= \langle O(B=0)\rangle_{gs}^{B=\infty}. \tag{14}$$

In comparison with other methods such as the renormalization group and perturbation theory, the Hilbert-space dimension remains completely in this method (contrary to the renormalization group), and this method can be used for strongly/weakly correlated systems (in contrast with the perturbation method, in which there must be a weak coupling parameter in the system's Hamiltonian). This method is also able to investigate the time evolution of a system [7, 33–42].

3. Accurate Solution of QIM in $-Jg\sigma_n^x$ Using CUTs

The QIM Hamiltonian in the constant transverse magnetic field $-Jg\sigma_n^x$ is given by

$$H = -J \sum_n \left(g\sigma_n^x + \sigma_n^z \sigma_{n+1}^z \right). \tag{15}$$

To accurately solve this model through CUTs, first by using Wigner–Jordan transformations [8]

$$\sigma_n^x = 1 - 2c_n^{\dagger} c_n. \tag{16}$$

$$\sigma_n^z = -\prod_{m<n} \left(1 - 2c_m^{\dagger} c_m\right) \left(c_n^{\dagger} + c_n\right) \tag{17}$$

and the Fourier transformation

$$c_k = \frac{1}{\sqrt{N}} \sum_n e^{ikna} c_n, \tag{18}$$

Eq. (15) is transformed into the spinless fermion form:

$$H = H_d + H_{nd}, \tag{19}$$

$$H_d = J \sum_k \left\{ 2\left[g - \cos(ka)\right] c_k^{\dagger} c_k - g \right\}, \tag{20}$$

$$H_{nd} = iJ \sum_k \sin(ka) \left(c_{-k}^{\dagger} c_k^{\dagger} - c_{-k} c_k \right). \tag{21}$$

In CUTs, since, for each component of the Hamiltonian matrix H, there is a flow, in which non-diagonal components tend to zero at the large enough values of B, all the coupling constants in (19) must be considered dependent on the momentum index. Doing so, in fact, there will be a particular series of coupling constants for each component of the Hamiltonian matrix. Because the flow varies in different components of the Hamiltonian matrix and depends on their energy, the flowing Hamiltonian is defined as

$$H(B) = H_d(B) + H_{nd}(B), \tag{22}$$

$$H_d(B) = \sum_k J_k(B) \left\{ 2\left[g_k(B) - \cos(ka)\right] c_k^{\dagger} c_k - g_k(B) \right\}, \tag{23}$$

$$H_{nd}(B) = i \sum_k J_k(B) \sin(ka) \left(c_{-k}^{\dagger} c_k^{\dagger} - c_{-k} c_k \right). \tag{24}$$

Employing the commutator of diagonal and non-diagonal Hamiltonian parts, the generator of CUTs is obtained as (we neglect to write the dependence of constants and parameters on B, for simplification):

$$\eta(B) = 2i \sum_k J_k (J_k + J_{-k}) \times$$
$$\times (g_k - \cos(ka)) \left(c_{-k}^{\dagger} c_k^{\dagger} - c_{-k} c_k \right). \tag{25}$$

Using this generator, the differential equations exhibiting the rescale of Hamiltonian's constants can be calculated as

$$[\eta_k, H_d] = -4i \sum_k \Big\{ J_k (J_k + J_{-k}) \times$$

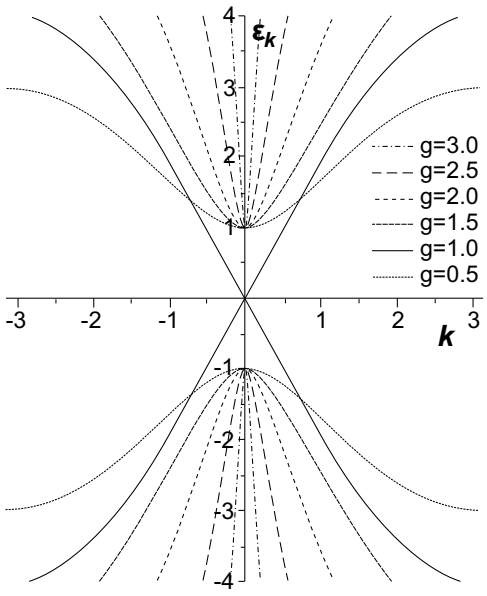

Fig. 1. Single-particle energies vs k for $g = 0.5$, 1, 1.5, 2.0, 2.5, and 3.0. Minimum energy gap at $g = 1$ and $k = 0$

$$\times (g_k - \cos(ka)) \sin(ka) \{J_{-k} (g_{-k} - \cos(ka)) +$$

$$+ J_k (g_k - \cos(ka))\} \left(c^\dagger_{-k} c^\dagger_k + c_{-k} c_k\right)\Big\}, \quad (26)$$

$$[\eta_k, H_{nd}] = -4i \sum_k \Big\{J_k (J_k + J_{-k}) \times$$

$$\times (g_k - \cos(ka)) \sin(ka) \{J_{-k} \sin(-ka) +$$

$$+ J_k \sin(ka)\} \left(c^\dagger_k c_k + c^\dagger_{-k} c_{-k} - 1\right)\Big\}. \quad (27)$$

Now, considering commutators (26) and (27), the flow equations can be obtained by equalizing the operators' coefficients on both sides of (10):

$$\frac{d}{dB} \{J_k (g_k - \cos(ka))\} = 2(J_k + J_{-k})^2 \sin(ka)^2 \times$$

$$\times \{J_{-k} (g_{-k} - \cos(ka)) + J_k (g_k - \cos(ka))\}, \quad (28)$$

$$\frac{dJ_k}{dB} = -4J_k (J_k + J_{-k}) \times$$

$$\times \{J_{-k} (g_{-k} - \cos(ka)) + J_k (g_k - \cos(ka))\}. \quad (29)$$

Regarding (28) and (29), if $k \to -k$, then $J_{-k} = J_k$ and $g_{-k} = g_k$. This result simplifies the differential equations. Equations (28) and (29) actually indicate the rescale of the parameters J and g in the 1D quantum Ising Hamiltonian. By simultaneously solving them and applying $J_k(B = 0) = J$ and $g_k(B = 0) = g$, we have

$$\lim_{B\to 0} \{J_k (g_k - \cos(ka))\} = \pm 2J \sqrt{g^2 - 2g\cos(ka) + 1}, \quad (30)$$

$$\lim_{B\to\infty} J_k(B) \to 0. \quad (31)$$

As is evident in (30) and (31), the coupling constant J approaches zero at the large enough values of B; consequently, the non-diagonal part of the Hamiltonian disappears. This means that the coefficient $2J(g - \cos(ka))$ is inserted and rescales the Hamiltonian's diagonal term to a new value. Using (30) and (31), the flowing Hamiltonian (diagonalized Hamiltonian) is obtained as

$$\tilde{H} = \sum_k \varepsilon_k \left(c^\dagger_k c_k - \frac{1}{2}\right), \quad (32)$$

where $\tilde{H} = H(B = \infty)$, and

$$\varepsilon_k = \pm 2J_0 \sqrt{g_0^2 - 2g_0 \cos(ka) + 1} \quad (33)$$

represents single-particle energies (SPEs) that were calculated by a different method in [1] (Fig. 1). The ground-state total energy and the first-excited energy are calculated to investigate QPT and to obtain the phase-transition critical point in this model. If we assume that there are only positive (negative) single-particle energies, there will not be any fermion (there will be full of fermions) in the ground eigenstate. Therefore, considering the flowing Hamiltonian (32), the ground-state energy is equal to

$$E_{gs} = \frac{-1}{2} \sum_k |\varepsilon_k|. \quad (34)$$

On the other hand, the excited states are created by occupying single-particle states (to empty single-particle states). Accordingly, the first excited state is created when a particle with the lowest single-particle energy occupies (empties) one of the single-particle states in the system's ground state. So the first-excited energy is obtained from: $E_{1\text{ex}} = E_{gs} + 2J|g - 1|$.

The diagrams of the ground-state and first-excited energies are plotted in Fig. 2. As observed, the energy gap is zero at $g_c = 1$, and the first-excited energy is tangent to the ground-state energy. Since there is a singularity in the higher-order derivatives of the ground-state energy with respect to the coupling constant g (Fig. 3), the phase transition in this system is a second-order QPT from ferromagnetic phase to paramagnetic phase. Considering (33) and the fact that the energy gap exponentially tends to zero near the critical point [1], we obtain

$$\Delta \propto J|g - g_c|^{vz}. \tag{35}$$

Therefore, the critical exponent vz equals zero for the QIM.

4. Calculation of $\langle \sigma_n^x \rangle$, $\langle \sigma_n^z \rangle$, and $C^x(j) = \langle \sigma_n^x \sigma_{n+j}^x \rangle - \langle \sigma_n^x \rangle^2$

First, the flow operators c_n and $c_n^\dagger$ must be obtained to calculate the expected values $\langle \sigma_n^x \rangle$ and $\langle \sigma_n^z \rangle$ and the correlation function $C^x(j)$. Based on (13), the flow equations for the creation and annihilation operators c_k and $c_k^\dagger$ are calculated as

$$\frac{dc_k(B)}{dB} = 8iJ^2(g - \cos(ka))\sin(ka)\, c_{-k}^\dagger(B), \tag{36}$$

$$\frac{dc_k^\dagger(B)}{dB} = -8iJ^2(g - \cos(ka))\sin(ka)\, c_{-k}(B). \tag{37}$$

By simultaneously solving (37) and (38), we have

$$c_k(B) = \frac{1}{2}\left(c_k(0) + c_{-k}^\dagger(0)\right)e^{i\Gamma_k(B)} +$$

$$+\frac{1}{2}\left(c_k(0) - c_{-k}^\dagger(0)\right)e^{-i\Gamma_k(B)}, \tag{38}$$

$$c_k^\dagger(B) = \frac{1}{2}\left(c_{-k}(0) + c_k^\dagger(0)\right)e^{-i\Gamma_k(B)} +$$

$$+\frac{1}{2}\left(c_k^\dagger(0) - c_{-k}(0)\right)e^{i\Gamma_k(B)}, \tag{39}$$

where $\Gamma_k(B) = \int_0^B 8J^2(g - \cos(ka))\sin(ka)\, dB'$. By considering (16), (17), (18), and the final Hamiltonian (32) as $|\Psi_{gs}\rangle = |0\rangle_{gs}^{B=\infty}$, the expected values can be obtained as

$$\langle \sigma_n^x \rangle_{gs}^{B=0} = \left\langle 1 - 2c_n^\dagger(\infty)\, c_n(\infty)\right\rangle_{gs}^{B=\infty} =$$

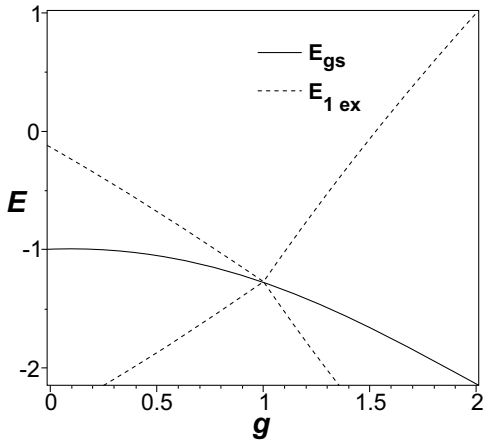

Fig. 2. Energy vs g (zero energy gap and second-order phase transition at $g_c = 1$)

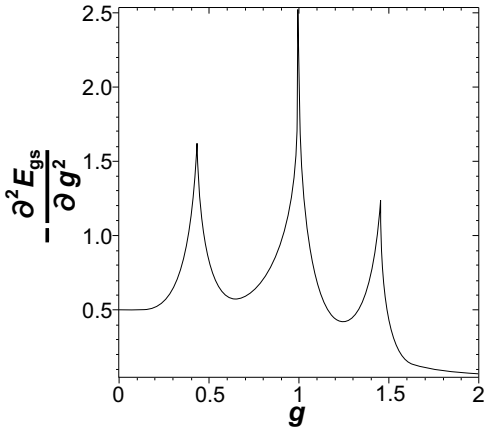

Fig. 3. Second derivative of the ground-state energy with respect to g

$$= \lim_{B,N\to\infty}\left\{1 - \frac{2}{n}\sum_k \sin(\Gamma_k(B))^2\right\} =$$

$$= 1 - \frac{a}{\pi}\int_{\frac{-\pi}{a}}^{\frac{\pi}{a}} dk \sin\left\{\frac{-i}{4}\ln\left(\frac{ge^{ika} - 1}{ge^{ika} - e^{2ika}}\right)2\right\} =$$

$$= \begin{cases} 0, & 0 \le g < 1, \\ 1 - \dfrac{1}{g^2}, & g \ge 1. \end{cases} \tag{40}$$

As can be seen, $\langle \sigma_n^x \rangle$ respectively tends to one and zero for $g \gg 1$ (in which most spins are oriented along the transverse field) and $g \ll 1$ (Fig. 4).

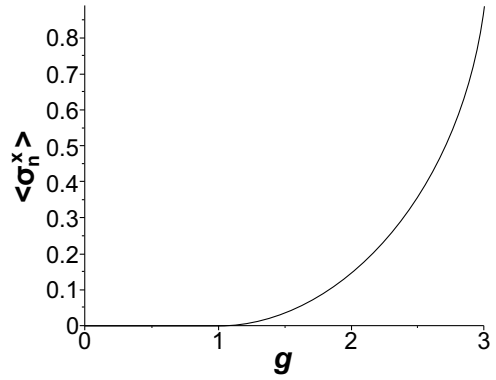

Fig. 4. Expected value $\langle\sigma_n^x\rangle$ vs g

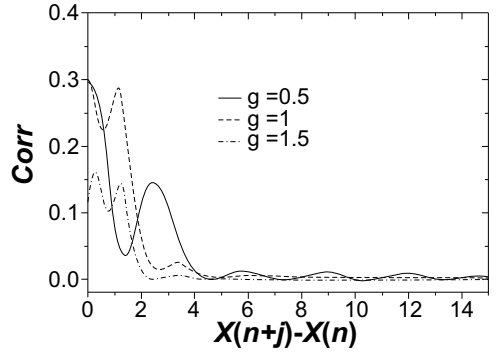

Fig. 5. Correlation function $C^x(j)$ vs the distance for $g = 0.5$, 1, and 1.5

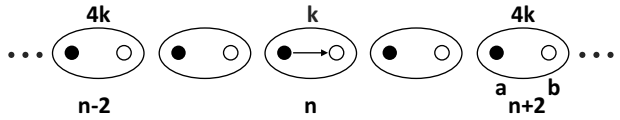

Fig. 6. Lattice structure of 1D QIM in $(-1)^n Jg\sigma_n^x$

Similarly for $\langle\sigma_n^z\rangle$:

$$\langle\sigma_n^z\rangle_{gs}^{B=0} = \left\langle -\prod_m \left(1 - 2c_m^\dagger(\infty)\, c_m(\infty)\right) \times \right.$$

$$\left. \times \left(c_n^\dagger(\infty) + c_n(\infty)\right)\right\rangle_{gs}^{B=\infty} = 0. \quad (41)$$

Because an odd number of c_k and $c_k^\dagger$ are multiplied by each other, the expected value $\langle\sigma_n^z\rangle$ becomes zero. This result is unexpected and far from our physical intuition, since the system's total magnetization is expected to be 1 or 0, at least at $g = 0$. The reason for this result is that since all the system's Hilbert space remains in the CUTs method, there are various states of the system for down and up spins. Hence, $\langle\sigma_n^z\rangle$ will be obtained in the zero space. Through a similar process for $C^x(j)$, we will have

$$C^x(j) = \left\{\frac{a}{2\pi}\int_{\frac{-\pi}{a}}^{\frac{\pi}{a}} \sin\left[2\tilde{F}_k\right]\sin(jka)\,dk\right\}^2 +$$

$$+\left\{\left(\frac{a}{2\pi}\right)^2 \int_{\frac{-\pi}{a}}^{\frac{\pi}{a}} \left(\cos\left[2\tilde{F}_{k_1}\right]\right)^2 \cos(jk_1a)\,dk_1 \times \right.$$

$$\left. \times \int_{\frac{-\pi}{a}}^{\frac{\pi}{a}} \left(\sin\left[2\tilde{F}_{k_2}\right]\right)^2 \cos(jk_2a)\,dk_2\right\}, \quad (42)$$

where

$$\tilde{F}_k = \lim_{B\to\infty}\left\{\int_0^B \Gamma_k(B')\,dB'\right\} = \frac{-i}{4}\ln\left(\frac{g - e^{-ika}}{g - e^{ika}}\right). \quad (43)$$

Through numerically solving (43), the spin correlation along the x-axis is achieved as Fig. 5. As is evident from the diagram, the spin correlation along x declines with increasing the distance, and it drops faster as the magnetic field rises; consequently, the long-range order in the system vanishes.

5. Accurate Solution of QIM in $(-1)^n Jg\sigma_n^x$ Using CUTs

We perform a similar procedure to solve the QIM Hamiltonian in the periodic magnetic field $(-1)^n Jg\sigma_n^x$ (Eq. (1)) through CUTs. First, the Wigner–Jordan and Fourier transformations are used, and then CUTs are employed in the Fourier space. But the difference is that each cell contains two atoms in this state. One atom senses $-Jg\sigma_n^x$, and the other senses $Jg\sigma_n^x$ (Fig. 6). Therefore, each atom's shift vector will become $2\mathbf{k}$ instead of $\mathbf{k}$. By applying the Wigner–Jordan transformation, relation (1) is transformed to the spinless fermion Hamiltonian below:

$$H = 2Jg\sum_n \left\{\left(c_n^\dagger c_n - \frac{1}{2}\right) - \left(d_n^\dagger d_n - \frac{1}{2}\right)\right\} -$$

$$- J\sum_n \left(c_n^\dagger d_n + d_n^\dagger c_n\right) - J\sum_n \left(d_n^\dagger c_{n+1} + c_{n+1}^\dagger d_n\right) -$$

$$- J\sum_n \left(c_n d_n + d_n c_n\right) - J\sum_n \left(d_n^\dagger c_{n+1}^\dagger + c_{n+1} d_n\right). \quad (44)$$

If a and b represent cell's fermions, $d_n^\dagger$ and d_n denote the creation and annihilation operators of a; $c_n^\dagger$ and c_n are the creation and annihilation operators of b in the n-th cell. Because this system's shift vector is $2\mathbf{k}$, the Fourier transforms of the creation and annihilation operators are as follows:

$$c_n = \frac{1}{N}\sum_k e^{2ikna} c_k, \tag{45}$$

$$c_n^\dagger = \frac{1}{N}\sum_k e^{-2ikna} c_k^\dagger. \tag{46}$$

Using these Fourier transforms, (45) is rewritten in the momentum space as

$$H = Jg\sum_k \left\{\left(c_k^\dagger c_k - \frac{1}{2}\right) - \left(d_k^\dagger d_k - \frac{1}{2}\right) + \text{h.c.}\right\} -$$
$$- \sum_k \left\{J\left(1 + e^{-2ika}\right) c_k^\dagger d_k + \text{h.c.}\right\} +$$
$$+ \sum_k \left\{J\left(-1 + e^{2ika}\right) c_{-k}^\dagger d_k + \text{h.c.}\right\}. \tag{47}$$

To obtain the single-particle energies through CUTs, an appropriate flowing Hamiltonian that contains all the possible square terms under appropriate initial conditions must be used. Considering the fact that terms such as $c_{-k}^\dagger c_k^\dagger + c_k c_{-k}$ or $d_{-k}^\dagger d_k^\dagger + d_k d_{-k}$ are produced during the flow process (calculating the commutators to obtain flow equations), we insert these terms into the Hamiltonian under the zero initial condition to consider such terms' effect on the rescale of the parameters of (1). Therefore, the flowing Hamiltonian we employed to solve through CUTs is

$$H(B) = H_0(B) + H_{\text{int}}(B), \tag{48}$$

where

$$H_0(B) = \sum_k \left\{\varepsilon_k^a(B)\left(c_k^\dagger c_k - \frac{1}{2}\right) +\right.$$
$$\left. + \varepsilon_k^b(B)\left(d_k^\dagger d_k - \frac{1}{2}\right)\right\}, \tag{49}$$

$$H_{\text{int}}(B) = \sum_k \left\{J_k(B) c_k^\dagger d_k + J_k^*(B) d_k^\dagger d_k\right\} +$$
$$+ \sum_k \left\{\alpha_k(B) c_{-k}^\dagger d_k^\dagger + \alpha_k^*(B) d_k c_{-k}\right\} +$$
$$+ \sum_k \left\{\beta_k(B) c_{-k}^\dagger c_k^\dagger + \beta_k^*(B) c_k c_{-k}\right\} +$$
$$+ \sum_k \left\{\gamma_k(B) d_{-k}^\dagger d_k^\dagger + \gamma_k^*(B) d_k d_{-k}\right\}. \tag{50}$$

To solve the flow equations, the initial conditions in (50) and (51) are defined as follows:

$$\alpha_k(0) = J(-1+e^{2ika}),\ J_k(0) = -J(1+e^{-2ika}), \tag{51}$$

$$\varepsilon_k^a(0) = 2Jg,\quad \varepsilon_k^b(0) = -2Jg,\quad \beta_k(0) = \gamma_k(0) = 0. \tag{52}$$

Performing the necessary calculations (see Appendix), the flow equations that rescale the Hamiltonian parameters include

$$\frac{d\varepsilon_k^a}{dB} = 2|J_k|^2\left(\varepsilon_k^a - \varepsilon_k^b\right) +$$
$$+ 2|\alpha_{-k}|^2\left(\varepsilon_k^a + \varepsilon_{-k}^b\right) + 2|\beta_k - \beta_{-k}|^2\left(\varepsilon_k^a + \varepsilon_{-k}^a\right), \tag{53}$$

$$\frac{d\varepsilon_k^b}{dB} = 2|J_k|^2\left(\varepsilon_k^a - \varepsilon_k^b\right) +$$
$$+ 2|\alpha_k|^2\left(\varepsilon_{-k}^a + \varepsilon_k^b\right) + 2|\gamma_k - \gamma_{-k}|^2\left(\varepsilon_k^b + \varepsilon_{-k}^b\right), \tag{54}$$

$$\frac{dJ_k}{dB} = -J_k\left(\varepsilon_k^a - \varepsilon_k^b\right)^2 +$$
$$+ \alpha_k^*\left(\beta_k - \beta_{-k}\right)\left(\varepsilon_k^a + \varepsilon_k^b + 2\varepsilon_{-k}^a\right) -$$
$$- \alpha_{-k}\left(\gamma_k^* - \gamma_{-k}^*\right)\left(\varepsilon_k^a + \varepsilon_k^b + 2\varepsilon_{-k}^b\right), \tag{55}$$

$$\frac{d\alpha_k}{dB} = -\alpha_k\left(\varepsilon_k^a + \varepsilon_k^b\right)^2 -$$
$$- J_k^*\left(\beta_k - \beta_{-k}\right)\left(2\varepsilon_k^a + \varepsilon_{-k}^a - \varepsilon_k^b\right) -$$
$$- J_{-k}\left(\gamma_k - \gamma_{-k}\right)\left(2\varepsilon_{-k}^b + \varepsilon_k^b - 2\varepsilon_{-k}^a\right), \tag{56}$$

$$\frac{d\beta_k}{dB} = -\beta_k\left(\varepsilon_k^a + \varepsilon_{-k}^b\right)^2 - J_k\alpha_k\left(\varepsilon_{-k}^a - \varepsilon_k^a + 2\varepsilon_k^b\right), \tag{57}$$

$$\frac{d\gamma_k}{dB} = -\gamma_k\left(\varepsilon_k^a + \varepsilon_{-k}^b\right)^2 - J_{-k}^*\alpha_k\left(\varepsilon_k^b - \varepsilon_{-k}^b + 2\varepsilon_{-k}^a\right). \tag{58}$$

These differential equations give us the rescale of the Hamiltonian parameters through CUTs. This

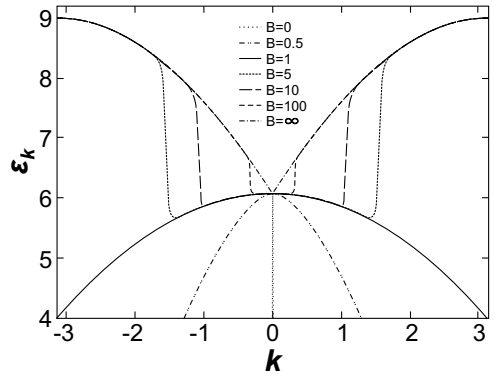

Fig. 7. Rescaled energy of atom a according to k for $J = 1$, $g = 0.5$, and a 200-site system

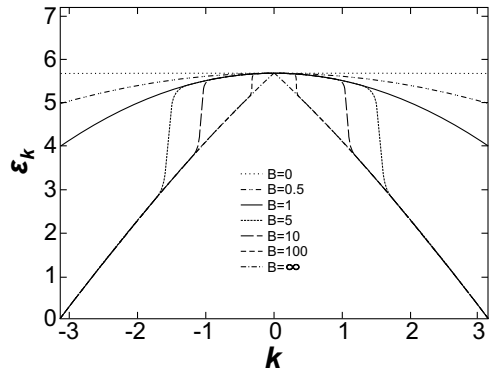

Fig. 8. Rescaled energy of atom b according to k for $J = 1$, $g = 0.5$, and a 200-site system

model's accurate energy spectrum is obtained by simultaneously numerically solving these coupled differential equations using the Runge–Kutta algorithm. The calculation results: all the non-diagonal part's parameters are rescaled to zero, and four values of single-particle energy are obtained for the atoms a and b (two values $\pm\varepsilon_k^a(\infty)$ for a and two values $\pm\varepsilon_k^b(\infty)$ for b) (Figs. 7 and 8). Accordingly, the final Hamiltonian (diagonalized Hamiltonian) that is obtained after an infinite number of ultrafine unitary transformations is as follows:

$$\tilde{H} = \sum_k \left\{\tilde{\varepsilon}_k^a c_k^\dagger c_k + \tilde{\varepsilon}_k^b d_k^\dagger d_k - \tilde{\varepsilon}_k^a - \tilde{\varepsilon}_k^b\right\}, \tag{59}$$

where $\tilde{H} = H(\infty)$, $\tilde{\varepsilon}_k^a = \varepsilon_k^a(\infty)$, and $\tilde{\varepsilon}_k^b = \varepsilon_k^b(\infty)$.

Note that, although a differential equation has several solutions, it has only one numerical solution. Hence, if we numerically solve the above equations, the non-physical solution $\varepsilon_k^a(\infty) = -\varepsilon_k^b(\infty)$ will be obtained. For this reason, to solve these equations, we add an extremely slight value 10^{-10} to $\varepsilon_k^a(B = 0)$ or $\varepsilon_k^b(B = 0)$ (the initial condition for solving differential equations). This numerical solution's results are plotted in Figs. 7, 8, and 9.

As can be observed, the negative energy levels are completely occupied by the fermions and the positive energy levels are empty. Therefore, depending on whether we consider the single-particle energies to be positive or negative, the system's ground state is completely empty or full of fermions, respectively. So that, a particle should be created or annihilated in the ground state to obtain the excited states. The energy required for a particle to move from the lower energy band to the higher empty energy band depends on the value of g so that it reaches its minimum for $g = 1$ at $k = 0$. Nevertheless, if we assume that $\varepsilon_k^{(a,b)} \geq 0$, considering (60), the total energies of the ground and first excited states will be obtained as follows:

$$E_{gs} = -\sum_k \left(\tilde{\varepsilon}_k^a + \tilde{\varepsilon}_k^b\right), \tag{60}$$

$$E_{1ex} = E_{gs} + \min\left\{\tilde{\varepsilon}_k^a, \tilde{\varepsilon}_k^b\right\}. \tag{61}$$

By studying the changes in the diagrams of E_{gs} and E_{1ex} versus g (Fig. 10), we can conclude that the energy gap is zero at the quantum critical point ($g_c = 1$) such that no level cutoff occurs. Moreover, it can be concluded from the energy-gap changes versus $|g - 1|$ that the critical exponent zv is equal to one. This indicates that this model is placed in the universality class of QIM. The investigation of the changes in the second-order derivative of the ground-state energy with respect to g shows that there is a singularity in this order of differentiation. So it is concluded that the phase transition at $g_c = 1$ is a second-order quantum phase transition from ferromagnetic phase to paramagnetic one.

6. Results and Discussion

This model is determined through a set of classical double-valued variables, $S_i = \pm 1$, so that S_i represents the spins placed on the lattice sites. This model's Hamiltonian is defined as

$$H = -J\sum_{\langle ij\rangle} S_i S_j - h\sum_i S_i, \tag{62}$$

where J denotes the interaction constant, and h is the external magnetic field. The parameters J and h are

constants with energy dimension. In the first term, $\langle ij\rangle$ represents the interaction of the nearest-neighbor spins. Here, if $J > 0$, the spin interaction will be ferromagnetic, otherwise, $J < 0$, antiferromagnetic.

Herein, the calculation method is divided into the high-temperature series expansion and the Padé approximation. First, the zero-field magnetic susceptibility is calculated through the high-temperature series expansion, and then the obtained series is analyzed in the Padé approximation. The series expansion method is a highly accurate approximation method used to calculate varios lattices' critical temperatures and exponents. The series expansion theory is applicable as a low/high-temperature approximation. To understand system's thermodynamic properties, its partition function should be calculated. Therefore, first using (63), the Ising-model partition function is obtained as

$$Z(K,h) = \sum_{\{S\}} e^{-\beta H} =$$

$$= \sum_{\{S\}} \exp\left(K \sum_{\langle ij\rangle} S_i S_j + \beta h \sum_i S_i\right), \qquad (63)$$

where the summation is performed over all the possible configurations of the system, $K = \beta J$ is a temperature-dependent coupling constant, and $\beta = 1/K_{\mathrm{B}}T$. At high temperatures, as T rises, K declines. Hence, the partition function can be expanded in K. Since $S_i S_j = \pm 1$ for the Ising model, the expression $e^{KS_iS_j}$ can be written as

$$e^{KS_iS_j} = (\cosh K)(1 + vS_iS_j), \qquad (64)$$

where $v = \tanh K$. Through a similar calculation procedure for the external field, the partition function is obtained as

$$Z_N(K) = (\cosh Kt)^{Nq/2}(\cosh \beta h)^N \times$$

$$\times \sum_{\{S\}} \prod\nolimits_{\langle ij\rangle} (1 + vS_iS_j) \times \prod\nolimits_K (1 + \tau S_K). \qquad (65)$$

The high-temperature expansion of Ising-model zero-field magnetic susceptibility is introduced as

$$\chi(v) = \beta^{-1} \lim_{h\to 0} \frac{\partial^2}{\partial h^2}\left(\frac{1}{N} \ln Z_N\right) =$$

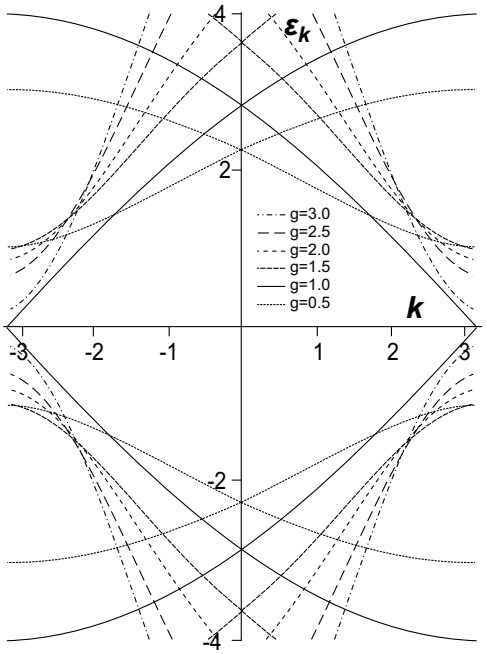

Fig. 9. Single-particle energies vs k for $g = 0.5$, 1, 1.5, 2.0, 2.5, and 3.0. Minimum energy gap at $g = 1$ and $k = 0$. Positive energy bands are empty, whereas negative energy bands are full of fermions

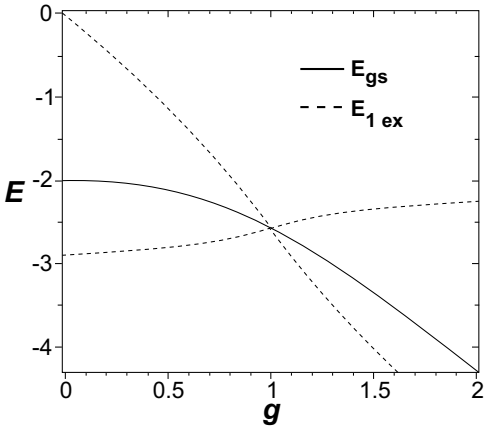

Fig. 10. Energy vs. g for QIM in $(-1)^n Jg\sigma_n^x$ (zero energy gap and 2^{nd}-order phase transition at $g_c = 1$)

$$= \frac{\beta}{NZ_N} \sum_{i,j} \sum_{\{S\}} S_iS_j e^{-\beta H}. \qquad (66)$$

Consequently, we have

$$\beta^{-1}\chi(v) = \frac{1}{N} \sum_{i,j} \langle S_iS_j\rangle = 1 + 2 \sum_{i\neq j} \langle S_iS_j\rangle, \qquad (67)$$

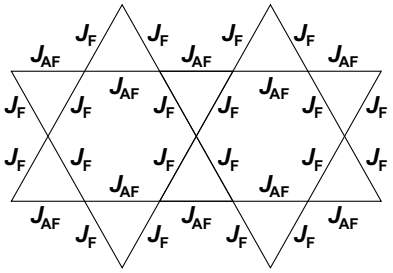

Fig. 11. Ising model with ferromagnetic and antiferromagnetic interactions on a kagome lattice

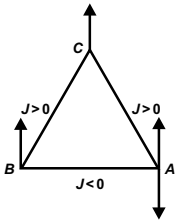

Fig. 12. If the spin A chooses the up/down direction, one of the interactions will not be satisfied. Therefore, this spin is frustrated to choose its direction

Table 1. **Critical temperature of the high-temperature expansion of the Ising-model magnetic susceptibility on a kagome lattice through the Padé approximation**

$[L, M]$	$x = -0.2$	$x = -0.3$	$x = -0.4$
$[6, 6]$	$K_{\rm B}T_{\rm C} \approx 1.316 J_{\rm F}$	$K_{\rm B}T_{\rm C} \approx 1.234 J_{\rm F}$	$K_{\rm B}T_{\rm C} \approx 0.793 J_{\rm F}$
$[5, 5]$	$K_{\rm B}T_{\rm C} \approx 1.316 J_{\rm F}$	$K_{\rm B}T_{\rm C} \approx 1.262 J_{\rm F}$	$K_{\rm B}T_{\rm C} \approx 0.819 J_{\rm F}$
$[4, 4]$	$K_{\rm B}T_{\rm C} \approx 1.234 J_{\rm F}$	$K_{\rm B}T_{\rm C} \approx 1.052 J_{\rm F}$	$K_{\rm B}T_{\rm C} \approx 0.840 J_{\rm F}$
$[3, 3]$	$K_{\rm B}T_{\rm C} \approx 1.262 J_{\rm F}$	$K_{\rm B}T_{\rm C} \approx 1.075 J_{\rm F}$	$K_{\rm B}T_{\rm C} \approx 0.884 J_{\rm F}$

Table 2. **Critical exponent of the high-temperature expansion of the Ising-model magnetic susceptibility on a kagome lattice through the Padé approximation**

$[L, M]$	$x = -0.2$	$x = -0.3$	$x = -0.4$
$[6, 6]$	$\gamma = 1.756$	$\gamma = 1.760$	$\gamma = 1.760$
$[5, 5]$	$\gamma = 1.770$	$\gamma = 1.770$	$\gamma = 1.767$
$[4, 4]$	$\gamma = 1.770$	$\gamma = 1.690$	$\gamma = 1.745$
$[3, 3]$	$\gamma = 1.752$	$\gamma = 1.770$	$\gamma = 1.700$

whose graphical expression is defined as

$$\beta^{-1}\chi(v) = \bar{\chi}(v) = 1 + 2\sum_{\{g_2\}} c(g) v^{l_g}, \tag{68}$$

where g_2 represents the graphs have two odd-degree vertexes, $c(g)$ is the graph immersion factor (called lattice constant), and l_g denotes the number of bonds pertaining to each graph. The analysis method varies based on what data is supposed to be obtained from the series. In this regard, there are various methods to analyze series. The Padé approximation method was first used for critical phenomena in 1961 [35]. The Padé approximation of the first N terms of an exponential series can be expressed as the division of two polynomials. As an example, for the first N terms of the function $F(x)$, the Padé approximation is written as

$$F(x) \cong \sum_{n=0}^{N} a_n x^n = \frac{P_L(x)}{Q_M(x)}, \tag{69}$$

where $P_L(x)$ and $Q_M(x)$ respectively represent polynomials of the order L and M such that $L + M \leq N$. The polynomial coefficients $P_L(x)$ and $Q_M(x)$ are determined by solving a set of linear equations. Employing such approximation, the analytical structure of series can be investigated and the function poles can be exactly determined. This procedure is as follows:

$$f(x) = A(x_C - x)^{-\theta}, \tag{70}$$

$$D \log F(x) \equiv \frac{f'(x)}{f(x)} = \frac{\theta}{x_C - x}. \tag{71}$$

Accordingly, the position of the singularity (critical) points can be obtained by estimating the roots of $Q_M(x)$, and thereby the critical exponent θ is evaluated. The magnetic susceptibility near the critical point is given by $\chi \sim |T - T_{\rm C}|^{-\gamma}$, where γ denotes the magnetic susceptibility critical exponent. Using the high-temperature expansion method, we study the magnetic susceptibility of an Ising-model zero field with first-neighbor interaction to ferromagnetic ($J_{\rm F}$) and antiferromagnetic ($J_{\rm AF}$) interactions on a kagome lattice. Such interaction is plotted in Fig. 11. The kagome lattice is a 2D non-Bravais frustrated spin system. This problem leads to an extreme complexity in the calculations. This model's zero-field magnetic susceptibility is calculated up to order 12 for different values of $J_{\rm AF}/J_{\rm F}$. Tables 1 and 2 show the calculation results.

If $-1 \leq J_{\rm AF}/J_{\rm F} \leq -0.2$, the zero-field magnetic susceptibility can be obtained through the high-temperature series expansion. Applying the Padé

approximation to the magnetic susceptibility series for $L = M$, the critical exponent and temperature of different states can be obtained. Tables 1 and 2 provide, respectively, the values obtained for the critical temperature and exponent for $J_{\rm AF}/J_{\rm F} = -0.2, -0.3, -0.4$, which is shown here by x.

As the tables indicate, the phase transition is observed for different values of antiferromagnetic interaction constant. In these three states, the phase temperature ($K_{\rm B}T_{\rm C}$) decreases with increasing the antiferromagnetic interaction constant (x). Also, these states' critical temperature is less than the transition temperature of the antiferromagnetic Ising model on a kagome lattice ($K_{\rm B}T_{\rm C} \approx 2.38$). Table 2 suggests that, according to the universality theory, these states' critical exponents are well consistent with the exact solution of the Ising model.

However, when $-1 \leq J_{\rm AF}/J_{\rm F} \leq -0.5$, the results obtained through the Padé approximation do not show any phase transition. The absence of a phase transition in such states is due to the fact that increasing the antiferromagnetic interaction constant strengthens this interaction and consequently leads to the spin confusion and magnetic frustration (see Fig. 12). Magnetic frustration or confusion is characterized as a state, in which a spin (or several) in a system cannot choose a direction completely satisfying all the interactions. In other words, the system cannot find a specific ground state for itself. Under such conditions, the system's ground state is several degenerate states, none of which is superior to others. Therefore, it can be said that the phase transition will not be observed in such systems due to the magnetic frustration.

7. Conclusions

In this paper, we have employed CUTs, as a new method for solving many-body quantum issues, to obtain the accurate energy spectrum of QIM in a constant magnetic field $-Jg\sigma_n^x$ and a periodic magnetic field $(-1)^n Jg\sigma_n^x$. As we expected, by varying the transverse magnetic field, both models showed the same results at the quantum critical point g_c, quantum phase type, and critical exponent zv. Furthermore, the calculation of the spin correlation function $C^x(j)$ has demonstrated that a rise in the transverse magnetic field does not cause a long-range order in the system. Also, the results of the high-temperature series expansion of the Ising-model zero-field magnetic susceptibility to antiferromagnetic and ferromagnetic interactions on a kagome lattice for the different values of antiferromagnetic interaction constant and through the Padé approximation indicate that when $J_{\rm AF}/J_{\rm F} = -0.2, -0.3, -0.4$, the ferromagnetic interactions dominate the antiferromagnetic interactions, and the phase transition is observed, consequently. These phase transition' critical exponent is well consistent with the exact solution of the Ising model. However, when $-1 \leq J_{\rm AF}/J_{\rm F} \leq -0.5$, the antiferromagnetic interactions compete with the ferromagnetic interactions. The results of application of the Padé approximation showed that no phase transition is observed in such systems due to the magnetic frustration.

The work was fully supported by grants from the Institute for Advanced Studies of Iran. The authors would like to express genuinely and sincerely the thanks and their acknowledgement to the Institute for Advanced Studies of Iran.

APPENDIX A.
Calculation of the flow equation for QIM in $(-1)^n Jg\sigma_n^x$ using CUTs

To calculate the generator, the diagonal part H_0 and non-diagonal part $H_{\rm int}$ are considered as follows:

$$H_0(B) = \sum_k \left\{ \varepsilon_k^a(B) \left(c_k^\dagger c_k - \frac{1}{2} \right) + \varepsilon_k^b(B) \left(d_k^\dagger d_k - \frac{1}{2} \right) \right\}, \quad \text{(A1)}$$

$$H_{\rm int}^{(1)}(B) = \sum_k \left\{ J_k(B)\, c_k^\dagger d_k + J_k^*(B)\, d_k^\dagger d_k \right\}, \quad \text{(A2)}$$

$$H_{\rm int}^{(2)}(B) = \sum_k \left\{ \alpha_k(B)\, c_{-k}^\dagger d_k^\dagger + \alpha_k^*(B)\, d_k c_{-k} \right\}, \quad \text{(A3)}$$

$$H_{\rm int}^{(3)}(B) = \sum_k \left\{ \beta_k(B)\, c_{-k}^\dagger c_k^\dagger + \beta_k^*(B)\, c_k c_{-k} \right\}, \quad \text{(A4)}$$

$$H_{\rm int}^{(4)}(B) = \sum_k \left\{ \gamma_k(B)\, d_{-k}^\dagger d_k^\dagger + \gamma_k^*(B)\, d_k d_{-k} \right\}, \quad \text{(A5)}$$

where $H_{\rm int} = H_{\rm int}^{(1)} + H_{\rm int}^{(2)} + H_{\rm int}^{(3)} + H_{\rm int}^{(4)}$.

1. Calculation of the generator of unitary transformations

$$\eta = \sum_k \left\{ J_k \left(\varepsilon_k^a - \varepsilon_k^b \right) c_k^\dagger d_k - \alpha_k \left(\varepsilon_{-k}^a + \varepsilon_k^b \right) c_{-k}^\dagger d_k + \right.$$
$$\left. + \beta_k \left(\varepsilon_k^a + \varepsilon_{-k}^a \right) c_{-k}^\dagger c^\dagger + \gamma_k \left(\varepsilon_k^b + \varepsilon_{-k}^b \right) d_{-k}^\dagger d_k^\dagger \right\} - \text{h.c.} \quad \text{(A6)}$$

2. Calculation of the commutator $[\eta, H_0]$

$$[\eta, H_0] = \sum_k \left\{ -J_k \left(\varepsilon_k^a - \varepsilon_k^b \right)^2 c_k^\dagger d_k - \alpha_k \left(\varepsilon_{-k}^a + \varepsilon_k^b \right)^2 \times \right.$$
$$\left. \times c_{-k}^\dagger d_k - \beta_k \left(\varepsilon_k^a + \varepsilon_{-k}^a \right)^2 c_{-k}^\dagger c^\dagger - \gamma_k \left(\varepsilon_k^b + \varepsilon_{-k}^b \right)^2 d_{-k}^\dagger d_k^\dagger \right\}. \quad \text{(A7)}$$

3. Calculation of the commutator $[\eta, H_{\rm int}^{(1)}]$

$$\left[\eta, H_{\rm int}^{(1)}\right] = \sum_k \left\{|J_k|^2 \left(\varepsilon_k^a - \varepsilon_k^b\right)\left(c_k^\dagger c_k - d_k^\dagger d_k -\right) - \right.$$
$$- \alpha_k(\varepsilon_{-k}^a - \varepsilon_k^b)\left(J_k c_{-k}^\dagger c_k^\dagger + J_{-k}^* d_{-k}^\dagger d_k^\dagger\right) -$$
$$- J_k^*\left(\varepsilon_k^a + \varepsilon_{-k}^b\right)(\beta_k - \beta_{-k})\, c_{-k}^\dagger d_k^\dagger -$$
$$\left. - J_{-k}\left(\varepsilon_k^b + \varepsilon_{-k}^b\right)(\gamma_k - \gamma_{-k})\, c_{-k}^\dagger d_k^\dagger\right\} + \text{h.c.} \quad \text{(A8)}$$

4. Calculation of the commutator $[\eta, H_{\rm int}^{(2)}]$

$$\left[\eta, H_{\rm int}^{(2)}\right] = \sum_k \left\{J_k\alpha_k\left(\varepsilon_k^a - \varepsilon_k^b\right) c_{-k}^\dagger c_k^\dagger - \right.$$
$$- J_{-k}\alpha_k^*\left(\varepsilon_{-k}^a - \varepsilon_{-k}^b\right) d_k d_{-k} + |\alpha_{-k}|^2\left(\varepsilon_k^a + \varepsilon_{-k}^b\right) c_k^\dagger c_k +$$
$$+ |\alpha_k|^2\left(\varepsilon_{-k}^a + \varepsilon_k^b\right) d_k^\dagger d_k + \alpha_k^*\left(\varepsilon_k^a + \varepsilon_{-k}^b\right)(\beta_k - \beta_{-k})\, c_k^\dagger d_k -$$
$$\left. - \alpha_{-k}^*\left(\varepsilon_k^b + \varepsilon_{-k}^b\right)(\gamma_k - \gamma_{-k})\, d_k^\dagger c_k - |\alpha_k|^2\left(\varepsilon_{-k}^a + \varepsilon_k^b\right)\right\} + \text{h.c.} \quad \text{(A9)}$$

5. Calculation of the commutator $[\eta, H_{\rm int}^{(3)}]$

$$\left[\eta, H_{\rm int}^{(3)}\right] = \sum_k \left\{-J_k\left(\varepsilon_k^a - \varepsilon_k^b\right)(\beta_k^* - \beta_{-k}^*)\, d_k c_{-k} + \right.$$
$$+ \alpha_k\left(\varepsilon_{-k}^a + \varepsilon_k^b\right)(\beta_k^* - \beta_{-k}^*)\, d_k^\dagger c_k +$$
$$+ |\beta_k - \beta_{-k}|^2\left(\varepsilon_k^a + \varepsilon_{-k}^a\right) c_k^\dagger c_k -$$
$$\left. - \beta_k(\beta_k^* - \beta_{-k}^*)\left(\varepsilon_k^a + \varepsilon_{-k}^b\right)\right\} + \text{h.c.} \quad \text{(A10)}$$

6. Calculation of the commutator $[\eta, H_{\rm int}^{(4)}]$

$$\left[\eta, H_{\rm int}^{(4)}\right] = \sum_k \left\{-J_k\left(\varepsilon_{-k}^a - \varepsilon_{-k}^b\right)(\gamma_k - \gamma_{-k})\, c_{-k}^\dagger d_k^\dagger - \right.$$
$$- \alpha_{-k}\left(\varepsilon_k^a + \varepsilon_{-k}^b\right)(\gamma_k^* - \gamma_{-k}^*)\, c_k^\dagger d_k +$$
$$+ |\gamma_k - \gamma_{-k}|^2\left(\varepsilon_k^b + \varepsilon_{-k}^b\right) d_k^\dagger d_k -$$
$$\left. - \gamma_k(\gamma_k^* - \gamma_{-k}^*)\left(\varepsilon_k^b + \varepsilon_{-k}^b\right)\right\} + \text{h.c.} \quad \text{(A11)}$$

1. S. Sachdev, *Quantum Phase Transitions* (Cambridge Univ. Press, Cambridge, 1999).
2. S. D. Glazek and K. Wilson, Phys. Rev. D **49**, 4214 (1994).
3. F. Wegner, Ann. Phys. Leipzig **3**, 77 (1994).
4. S. Kehrein, *The Flow Equation Approach to Many-Particle Systems* (Springer, Berlin, 2006).
5. F. Wegner, Phys. Rep. **348**, 77 (2001).
6. S. Dusuel and G. Uhrig, J. Phys. A **37**, 9275 (2005).
7. A. Hackl and S. Kehrein, Phys. Rev. B **78**, 092303 (2008).
8. P. Jordan and E. Wigner, Z. Phys. **47**, 631 (1928).
9. J. Dziarmaga, Phys. Rev. Lett. **95**, 245701 (2005).
10. A. Leclair, F. Lesage, S. Sachdev, and H. Saleur, Nucl. Phys. B **482**, 579 (1996).
11. S. A. Pikin and V. M. Tsukernik, Sov. Phys. JETP **23**, 914 (1966).
12. E. Barrouch and B.M. McCoy, Phys. Rev. A **3**, 786 (1971).
13. J. Perk, H.W. Capel, M.J. Zuilhof, and Th.J. Siskens, Physica A **81**, 319 (1975).
14. T. Barnes, E. Dogotto, J. Riera, and E.S. Swanson, Phys. Rev. B **47**, 3196 (1993).
15. E. Dagotto and T.M. Rice, Science **271**, 618 (1996).
16. P. Lecheminant, Cond-mat / 0306520, 60 (2003).
17. H.J. Schulz, Phys. Rev. B **34**, 6372 (1986).
18. R. M. Wiessner, Phys. Rev. B **60**, 6545 (1999).
19. T. Vekua, G.I. Japaridze, and H.J. Mikeska, Phys. Rev. B **67**, 064419 (2003).
20. T. Vekua, G.I. Japaridze, and H.J. Mikeska, Phys. Rev. B **70**, 014425 (2004).
21. J.C. Cullum and R.A. Willoughby, *Lanczos Algorithms for Large Symmetric Eigenvalue Computations* (Birkhäuser, Boston, 1985).
22. B.N. Parlett, *The Symmetric Eigenvalue Problem* (Prentice-Hall, Englewood Cliffs, 1980).
23. R. Hogemans, J.S. Caux, and U. Low, Phys. Rev. B **71**, 011137 (2005).
24. M. Vojta, Rep. Prog. Phys. **66**, 2069 (2003).
25. K.I. Kugel and D.I. Khomskii, Sov. Phys. JETP **37**, 725 (1973).
26. B.M. Doucot, V. Fiegelman, L.B. Loffe, and A.S. Ioselevich, Phys. Rev. B **71**, 02405 (2005).
27. E. Eriksson and H. Johannesson, Phys. Rev. B **79**, 224424 (2009).
28. W. Brzezicki, J. Dziamaga, and A.M. Oles, Phys. Rev. B **75**, 134415 (2007).
29. W. Brzezicki and A.M. Oles, Acta Phys. Pol. A **115**, 162 (2009).
30. K.W. Sun, Phys. Rev. B **80**, 174417 (2009).
31. C. Lanczos, J. Res. Natl. Bur. Stand. **45**, 255 (1950).
32. H.Q. Lin and J.E. Gubernatis, Comput. Phys. **7**, 400 (1993).
33. J. Oitmaa, C. Hamer, and W. Zheng, *Series Expansion Methods for Strongly Interacting Lattice Models* (Cambridge Univ. Press, New York, 2006).
34. N. Goldenfeld, *Lectures on Phase Transitions and the Renormalization Group* (Addison-Wesley, New York, 1992).
35. R. Szymczak, M. Baran, J.F. Finowicki, B. Krzymanska, P. Aleshkevych, and H. Szymczak, Acta. Phys. Polon. A **113**, 413 (2007).
36. C.T. Tseng, and K.Y. Lin, J. Chinese. Phys. **34**, 1254 (1996).
37. M.L. Bellac, Quantum and Statistical Field Theory, (Oxford Univ. Press, New York, 1991).
38. J.M. Yeomans, *Statistical Mechanics of Phase Transitions*, (Oxford Univ. Press, New York, 1992).
39. J.M. Chen and K.Y. Lin, Chin. Phys. **34**, 1156 (1996).
40. Y.C. Hsiao and K.Y. Lin, Phys. A **252**, 211 (1998).
41. G. Nandhini and M.V. Sangaranarayanan, e-print arXiv:0801.0662v1. [Cond-Mat.Stat-Mech] (2008).
42. R.A. Farrell, Phys. Rev. **180**, 579 (1969).

Received 31.05.12

А. Хейдарі, Ф. Горбані, М. Горбані

НОВИЙ МЕТОД ДОСЛІДЖЕННЯ
І ТОЧНОГО РОЗВ'ЯЗАННЯ ОДНОВИМІРНОЇ
КВАНТОВОЇ МОДЕЛІ ІЗІНГА ДЛЯ ПОСТІЙНОГО
І ЗМІННОГО ПОПЕРЕЧНИХ
МАГНІТНИХ ПОЛІВ

Р е з ю м е

Одновимірна квантова модель Ізінга (1КМІ) описує квантові фазові переходи із взаємодією найближчих сусідів в постійному магнітному полі. Раніше було розроблено ряд методів точного розв'язання 1КМІ. Застосовуючи неперервне унітарне перетворення як новий аналітичний метод опису багаточастинкових систем, ми вперше отримали розв'язок 1КМІ для постійного і для регулярного (періодичного) поперечних магнітних полів. Як і очікувалося, критичні індекси є такими самими, що і в точних розв'язках. Застосовуючи наближення Паде і розвинення в ряд у границі високих температур, ми вивчили сприйнятливість моделі Ізінга без магнітного поля з антиферомагнітною взаємодією на ґратці кагоме. Показано, що при зміні константи антиферомагнітної взаємодії фазовий перехід виникає за умови $J_{\mathrm{AF}}/J_{\mathrm{F}} > -0.5$. Згідно з теорією універсальності, критичні індекси для таких систем добре узгоджуються з індексами в моделі Ізінга.